OXFORD

JNCI J Natl Cancer Inst (2017) 109(11): djx062

doi: 10.1093/jnci/djx062
First published online August 28, 2017
Article

ARTICLE

Loss of DNA Damage Response in Neuroblastoma and Utility of a PARP Inhibitor

Masatoshi Takagi*, Misa Yoshida*, Yoshino Nemoto*, Hiroyuki Tamaichi, Rika Tsuchida, Masafumi Seki, Kumiko Uryu, Rina Nishii, Satoshi Miyamoto, Masahiro Saito, Ryoji Hanada, Hideo Kaneko, Satoru Miyano, Keisuke Kataoka, Kenichi Yoshida, Miki Ohira, Yasuhide Hayashi, Akira Nakagawara, Seishi Ogawa, Shuki Mizutani, Junko Takita

Affiliations of authors: Department of Pediatrics and Developmental Biology (MT, YN, RT, RN, SMiyam, SMizut), Tokyo Medical and Dental University, Tokyo, Japan; Department of Pediatrics, Graduate School of Medicine (MY, MSe, KU, JT), Laboratory of DNA Information Analysis, Human Genome Center, Institute of Medical Science (SMiyan), Laboratory of Sequence Analysis, Human Genome Center, Institute of Medical Science (SMiyan), The University of Tokyo, Tokyo, Japan; Department of Pediatrics and Adolescent Medicine, School of Medicine, Juntendo University, Tokyo, Japan (HT, MSa); Department of Pediatric Hematology/Oncology, Saitama Children's Medical Center, Saitama, Japan (RH), Department of Pediatrics, Nagara Medical Center, Gifu, Japan (HK); Department of Pathology and Tumor Biology, Kyoto University, Kyoto, Japan (KK, KY, SO); Division of Cancer Genomics, Saitama Cancer Center Research Institute, Saitama, Japan (MO); Division of Cancer Genomics, Chiba Cancer Center, Chiba, Japan (MO, AN); Gunma Children's Medical Center, Gunma, Japan (YH); Saga Medical Center, Saga, Japan (AN).

*Authors contributed equally to this work.
For the full list of authors and affiliations, see the Notes section.
Correspondence to: Masatoshi Takagi, MD, PhD, Departments of Pediatrics and Developmental Biology, Graduate Medical School, Tokyo Medical and Dental University, 1-5-45, Yushima, Bunkyo-ku, Tokyo 113-8519, Japan (e-mail: m.takagi.ped@tmd.ac.jp); or Junko Takita, MD, PhD, Department of Pediatrics, Graduate School of Medicine, The University of Tokyo, 7-3-1, Hongo, Bunkyo-ku, Tokyo 113-8655, Japan (e-mail: jtakita-tky@umin.ac.jp).

Abstract

Background: Neuroblastoma (NB) is the most common solid tumor found in children, and deletions within the 11q region are observed in 11% to 48% of these tumors. Notably, such tumors are associated with poor prognosis; however, little is known regarding the molecular targets located in 11q.
Methods: Genomic alterations of *ATM*, DNA damage response (DDR)–associated genes located in 11q (*MRE11A, H2AFX*, and *CHEK1*), and *BRCA1, BARD1, CHEK2, MDM2*, and *TP53* were investigated in 45 NB-derived cell lines and 237 fresh tumor samples. PARP (poly [ADP-ribose] polymerase) inhibitor sensitivity of NB was investigated in in vitro and in vivo xenograft models. All statistical tests were two-sided.
Results: Among 237 fresh tumor samples, *ATM, MRE11A, H2AFX*, and/or *CHEK1* loss or imbalance in 11q was detected in 20.7% of NBs, 89.8% of which were stage III or IV. An additional 7.2% contained *ATM* rare single nucleotide variants (SNVs). Rare SNVs in DDR-associated genes other than *ATM* were detected in 26.4% and were mutually exclusive. Overall, samples with SNVs and/or copy number alterations in these genes accounted for 48.4%. ATM-defective cells are known to exhibit dysfunctions in homologous recombination repair, suggesting a potential for synthetic lethality by PARP inhibition. Indeed, 83.3% NB-derived cell lines exhibited sensitivity to PARP inhibition. In addition, NB growth was markedly attenuated in the xenograft group receiving PARP inhibitors (sham-treated vs olaprib-treated group; mean [SD] tumor volume of sham-treated vs olaprib-treated groups = 7377 [1451] m^3 vs 298 [312] m^3, $P = .001$, n = 4).
Conclusions: Genomic alterations of DDR-associated genes including ATM, which regulates homologous recombination repair, were observed in almost half of NBs, suggesting that synthetic lethality could be induced by treatment with a PARP inhibitor. Indeed, DDR-defective NB cell lines were sensitive to PARP inhibitors. Thus, PARP inhibitors represent candidate NB therapeutics.

Received: November 15, 2016; **Revised:** December 25, 2016; **Accepted:** March 13, 2017

© The Author 2017. Published by Oxford University Press. All rights reserved. For Permissions, please e-mail: journals.permissions@oup.com.

Downloaded from https://academic.oup.com/jnci/article/109/11/djx062/4096548 by guest on 24 April 2024

Advanced neuroblastoma (NB) is one of the most intractable childhood cancers (1). *MYCN* amplification is a well-characterized genetic alteration in NB that directly associates with advanced disease and poor prognosis. In addition to *MYCN* amplification, several other genome alterations are associated with NB. Mosse et al. and our group reported that activating mutations in the tyrosine kinase domain of the *ALK* oncogene account for 2% of familial NB and 5% to 10% of sporadic NB cases (2,3). Genome-wide association studies have identified single nucleotide variants (SNVs) within the putative gene *FLJ22536* in chromosome band 6p22.3, *BARD1* in 2q35, and *LMO1* in 11p15.4 that are associated with development of NB (4–6). In addition to gene mutations, genome copy alterations are also implicated in NB; for example, an unbalanced gain of 17q is observed in approximately half of NBs. Loss of 1p, 3p, and 11q is also observed in the advanced stage of NB and is associated with an unfavorable prognosis (7–9). Deletion of 11q is observed in 11% to 48% of NB cases; these cases, which fall into distinct genetic subtypes, exhibit no *MYCN* amplification (10,11). However, little is known about the molecular target(s) located in 11q. *CADM1* was identified as a candidate gene in 11q23 in NB (12,13). The 11q21-24 is unique in cancer genetics because it contains many cancer-associated genes in addition to *CADM1*, including *MRE11A, ATM, KMT2A, H2AFX, CBL, CHEK1, ETS1, FLI1*, and *TP53AIP1*.

DNA damage response (DDR) is crucial for maintenance of genome integrity. ATM is a master regulator of DDR, and various other molecules involved in the DDR are regulated via ATM. For example, CHEK1 is a signaling molecule that activates the G2/M cell cycle checkpoint, and H2AFX is a histone that functions specifically during DNA damage. In addition, ATM plays a critical role in DNA repair in both the nonhomologous end-joining (NHEJ) and homologous recombination repair (HRR) pathways (14–17). Cells constantly undergo DNA damage caused by agents such as oxygen-free radicals and natural ionizing radiation. Therefore, cellular DNA in mammalian cells is under constant DNA-damaging stress, posing the risk of mutation. DNA damage is sensed by ATM and ATR, which upon activation initiate DDR pathways and trigger cell cycle checkpoints, apoptosis, or the DNA repair machinery (18). Thus, the DDR is the most important factor in maintaining genome integrity. However, once DNA damage occurs in genes that play a crucial role in the DDR itself, the checkpoint pathway is compromised; as a result, cells acquire a growth advantage and can undergo transformation more readily. Such cells, which are genomically unstable, start to proliferate and accumulate additional complex mutations, contributing to the stepwise evolution of tumorigenesis (19–22). MYC activation activates the ATM-dependent DDR pathway and CDKN2A-dependent pathway (23,24). In addition, ATM exerts a tumor suppressor function through MYC (25). Thus, ATM and MYC act in the same circuit in the context of tumorigenesis and tumor suppression.

In this study, we investigated the role of *ATM* and DDR-associated molecules located in 11q, *MRE11A, H2AFX, and CHEK1, as well as BRCA1, BARD1, CHEK2, MDM2,* and *TP5*.

Methods

Samples and Cell Lines

The SJNB series and the UTP-N-1 cell lines were gifts from A. T. Look (Dana-Farber Cancer Institute) and A. Inoue (St. Jude Children's Research Hospital), respectively. The PFSK-1, MC-IXC, KAN-TS, SK-PN-DW, KELLY, and CHP-212 lines were gifts from Astellas Pharma, Inc. (Tokyo, Japan). The other cell lines used were obtained from the JCRB Cell Bank and the RIKEN BioResource Center. The SV40-transformed wild-type cell line GM0637 and AT cell line GM05849C (7009 del TG) were obtained from Coriell Cell Repositories (Camden, NJ). Cells were maintained at approximately 5×10^5 cells per mL in DMEM (Life Technologies) containing 10% fetal calf serum (FCS) at 37 °C in 5% CO_2. The discovery and validation cohorts comprised 78 and 159 NB tumor samples, respectively, from different subjects. The discovery cohort consisted of samples diagnosed between 1996 and 2002 and obtained from the Chiba Cancer Center tissue bank. The validation cohort consisted of samples diagnosed between 1990 and 2012, obtained from the Tokyo University and JNBSG (Japan Neuroblastoma Study Group). No samples overlapped between the two cohorts. The patients were staged according to the International NB Staging System (1). The clinical information is summarized in Supplementary Table 1 (available online).

Fresh tumor samples were obtained during surgery or biopsy from patients who were initially diagnosed with NB and admitted to a number of hospitals in Japan. Relapsed samples were not included in this study. Written informed consent for sample research use was obtained from the parents of the patients. This study was approved by the Human Genome, Gene Analysis Research Ethics Committee of the University of Tokyo (Approved No. 1598-9), the ethical committee of Tokyo Medical and Dental University (Approved No. 4 and 103), and Chiba Cancer Center (Approved No. 19-9 and 444). To confirm the somatic/germline origins of the detected mutations, corresponding normal specimens (mononuclear cells from peripheral blood or bone marrow with no tumor cells) from nine subjects with NB were also analyzed. To evaluate SNVs of *ATM* in a healthy Japanese cohort, mononuclear cells from the peripheral blood of 171 healthy volunteers were also used.

DNA Sequencing

DNA sequencing was performed by target sequencing using the HiSeq 2000 or MiSeq platform (Illumina, San Diego, CA). Primers were designed to cover the entire coding exons of *ATM* and other DDR-associated genes (Supplementary Table 2, available online).

Animal Studies and Tumor Xenografts

All animal care procedures were carried out in accordance with institutional guidelines approved by Tokyo Medical and Dental University (Tokyo, Japan). All mice were kept in a pathogen-free unit in the vivarium of Tokyo Medical and Dental University. Eight-week-old female NSG mice (Charles River, Yokohama, Japan) were anesthetized, and 1×10^7 SK-N-DZ or SK-N-SH cells were injected subcutaneously into the back skin for xenografts. Oral administration of the PARP inhibitor (50 mg/kg body weight) was initiated on day 2 and continued every other day, three times a week, for a total of three weeks. The same volume of the carrier used to dissolve the PARP inhibitor was administered orally in controls. Tumor volume was measured every two to three days.

Data Analysis

Evaluation of SNVs was performed using public source databases. Polymorphism and allele frequency of SNVs were

Downloaded from https://academic.oup.com/jnci/article/109/11/djx062/4096548 by guest on 24 April 2024

Table 1. Genome alteration of ATM and DDR-associated molecules in neuroblastoma*

	Copy number loss or uniparental disomy				Nucleotide alteration
Cohort	*ATM*	*H2AFX*	*CHEK1*	*MRE11A*	ATM
Cell lines, % (n/total)	35.6 (16/45)	30.8 (12/39)	28.2 (11/39)	23.0 (9/39)	11.1 (5/45)
Discovery, % (n/total)	14.1 (11/78)	NA	NA	NA	10.3 (8/78)
Validation, % (n/total)	18.2 (29/159)	18.8 (30/159)	18.2 (29/159)	17.6 (28/159)	5.7 (9/159)

*23.9% (38/159) of cases harbored deletion of *ATM*, *H2AFX*, *CHEK1*, or *MRE11A*. DDA = DNA damage response; NA = not analyzed.

determined using dbSNP build 131/132, 1000 Genomes Project, and the Human Genetic Variation database (HGVD).

The Methods for Survival Curves

Survival curves were constructed according to the methods of Kaplan and Meier. The time to an event for the overall survival analysis was calculated as the time from first diagnosis until the time of death or the time of last contact if the patient was alive.

Statistical Analysis

P values were calculated by Mann-Whitney U test for DR-GFP assay. Tumor volumes from the mouse experiments were analyzed using the Student's *t* test. Comparisons of the survival curves were performed with a log-rank test. All statistical tests were two-sided, and a *P* value of less than .05 was considered statistically significant.

Detailed information regarding the other methods is available in the Supplementary Materials and Methods (available online).

Results

Copy Number Alteration of ATM and Other DDR-Associated Genes in NB

Approximately 14% to 48% of NB cases are associated with loss or imbalance of 11q, the site of the ATM locus (10,11,26). Accordingly, we investigated genomic copy number alteration of the *ATM* gene in NB-derived cell lines. Of the 45 cell lines examined, 12 exhibited *ATM* deletion and four exhibited uniparental disomy (UPD; total 35.6%) (Supplementary Table 3 and Supplementary Figure 1, available online); Multiplex ligation-dependent probe amplification (MLPA) and fluorescence in situ hybridization (FISH) analysis also supported these findings (Supplementary Figure 1, B and C, available online). Comprehensive copy number analysis in 39 cell lines revealed that the DDR-associated molecules *H2AFX*, *CHEK1*, and *MRE11A* were deleted with almost the same frequency as *ATM* (Table 1; Supplementary Figure 1, available online).

These observations in cell lines prompted us to investigate further using clinical samples. Initially, 78 fresh NB samples were screened as a discovery cohort. Loss of the *ATM* locus was observed in 14.1% (11/78) of tumor samples. Furthermore, 22.2% (10/45) of stage III and IV cases had lost *ATM*, indicating that 90.9% (10/11) of *ATM*-deleted cases were stage III or IV (Table 1). To further confirm these observations, we performed comprehensive copy number analysis using an additional 159 fresh NB tumor samples as a validation cohort. Loss or UPD of 11q, including deletion or UPD of *ATM*, *H2AFX*, *CHEK1*, and *MRE11A*, was observed in 23.9% of these samples (38/159), and 89.5% (34/38) of 11q imbalanced cases were stage III or IV (Table 1 and Figure 1A). In total *ATM*, *MRE11A*, *H2AFX*, and/or *CHEK1* loss or imbalance in 11q was detected in 20.7% (49/237) of NBs, 89.8% (44/49) of which were stage III or IV. Statistically significant copy number gains or losses were evaluated by GISTIC algorithms using 133 fresh NB samples (27). Locus amplification of *MYCN* (2p25.1–2p21), *MDM2* (12q15), and 17q12–17q25 exhibited low *q* values. Among the loci exhibiting low *q* values, regions 11q22.1 to 11q24.3 contained the DDR-associated genes *MRE11A*, *ATM*, *H2AFX*, and *CHEK1* (Figure 1, B and C).

ATM Gene Alteration in NB

Subsequently, *ATM* gene mutations were investigated using 45 NB-derived cell lines. Sequencing analysis identified five *ATM* SNVs (Table 1; Supplementary Table 3, available online). V2716A, identified in the IMR-32 line, is located in the ATP-binding site within the catalytic domain of ATM and was previously characterized as a pathogenic dominant-negative mutation in a family exhibiting mild ataxia telangiectasia (28,29). IMR-32 also harbored UPD of the *ATM* locus, rendering the cells homozygous for *ATM* mutation. Notably, GOTO cells harbored deletion of 11q, including the *ATM* region along with a nonsense mutation in the *ATM* gene, rendering the cells *ATM*-null.

To further confirm these observations, we analyzed clinical fresh NB tumor samples. Seven *ATM* nonsynonymous SNVs in six subjects and two intragenic deletions were identified in the 78 fresh NB samples comprising the discovery cohort (7.6% and 2.6% of subjects, respectively; total = 10.2%) (Table 1; Supplementary Table 4, available online). Except in one case, all nucleotide changes were identified as germline variants. In addition, nonsynonymous *ATM* SNVs were identified in 5.7% (9/159) of samples in the validation cohort (Table 1; Supplementary Table 4, available online). The status of germline variants was not investigated in all cases, but two cases were confirmed as germline SNVs, and data from allele frequency estimation suggested that seven of nine SNVs were germline mutations. Overall, nonsynonymous *ATM* SNVs were identified in 7.2% (17/237) of fresh NB samples, and 58.8% (10/17) of the cases in which nonsynonymous *ATM* SNVs were identified were stage III and IV NB. *ATM* SNVs were dispersed throughout the entire *ATM* region (Supplementary Figure 2A, available online). Among them, V2716A and K2749I mutations were both identified in the region encoding the ATM catalytic domain. Notably, in fresh tumor samples, *ATM* SNVs and 11q loss were mutually exclusive (Figure 2A).

DDR-Associated Gene Alteration in Fresh NB Samples

Target sequencing using 39 NB-derived cell lines and a COSMIC database search identified six nonsynonymous SNVs of

Downloaded from https://academic.oup.com/jnci/article/109/11/djx062/4096548 by guest on 24 April 2024

ARTICLE

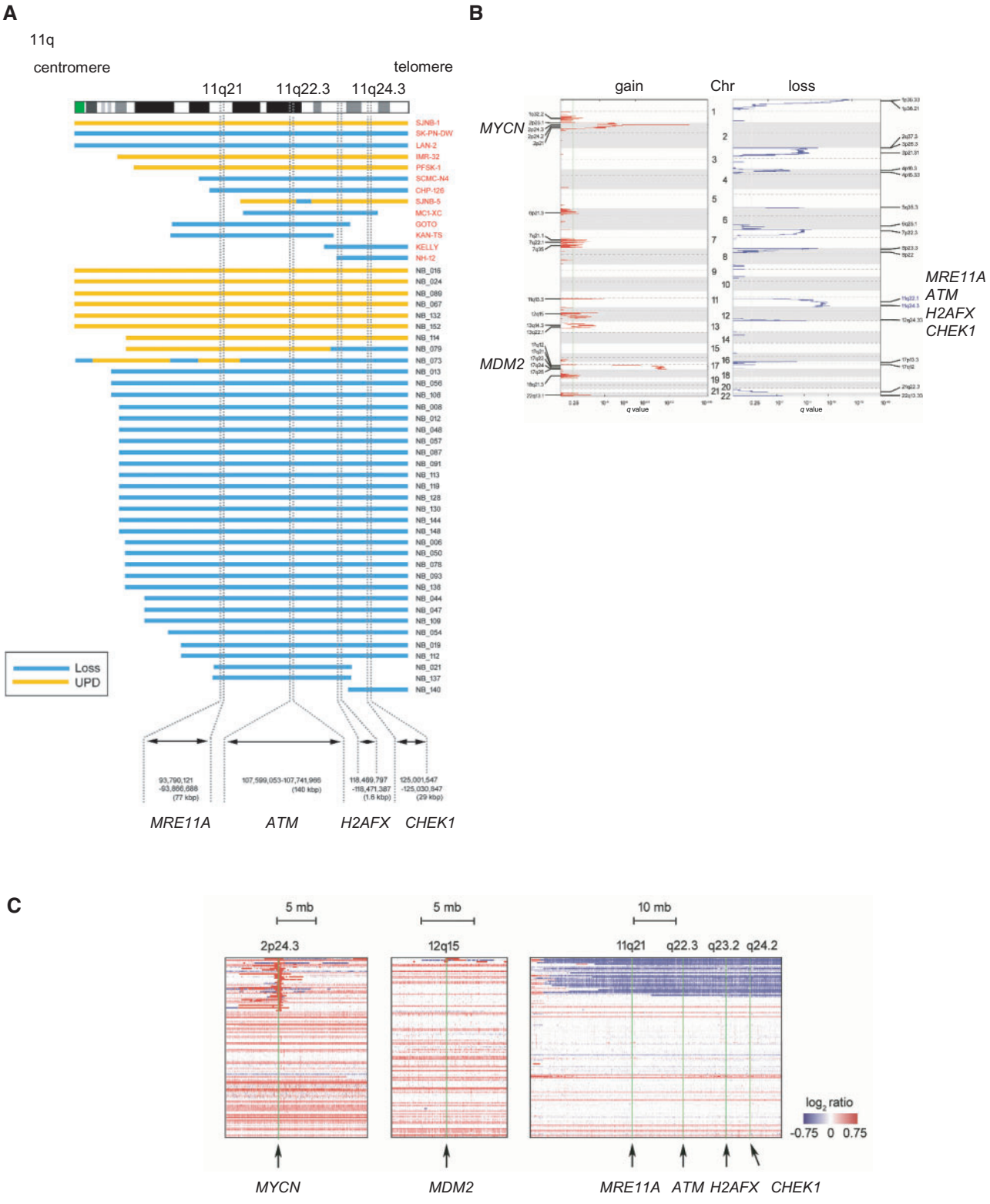

Figure 1. Statistically significant copy number alterations in clinical neuroblastoma (NB) specimens. **A)** Overall representation of 11q loss of heterozygosity observed in NB tumors of the validation cohort (n = 159). **Blue bars** indicate loss, and **orange bars** indicate uniparental disomy. **B)** Regions with statistically significant copy number gains and losses, as detected by the GISTIC algorithm, are shown in the **left and right boxes**, respectively. Putative gene targets are listed for each *q* value peak. A **dashed line** represents the centromere of each chromosome. **Red and blue lines** indicate the *q* values for gains and losses, respectively. **C)** Log-ratio copy number heat maps are shown for regions at 2p24.3, 12q15, and 11q. Kbp = kilo base pairs; UPD = uniparental disomy.

ARTICLE

Downloaded from https://academic.oup.com/jnci/article/109/11/djx062/4096548 by guest on 24 April 2024

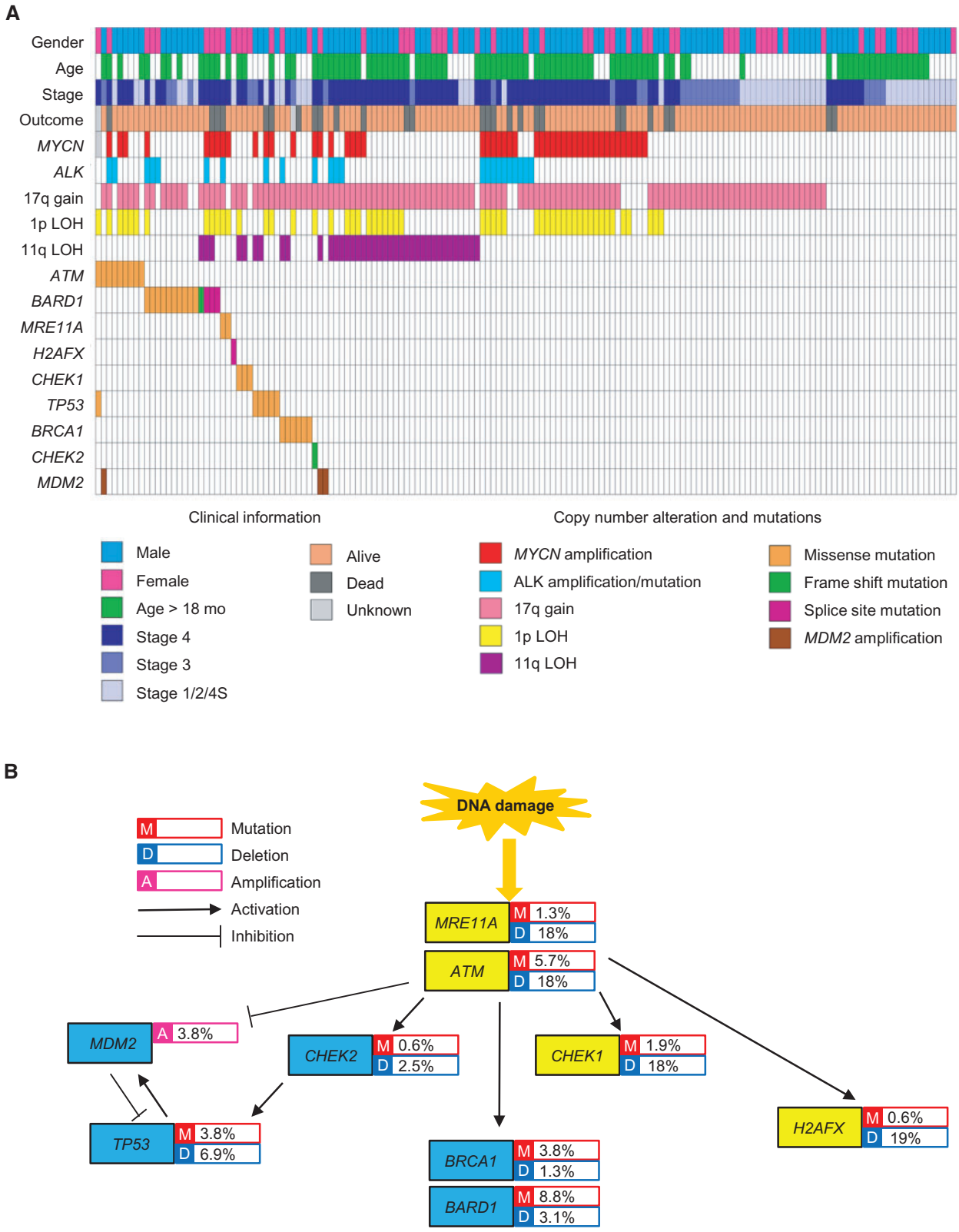

Figure 2. Analysis of neuroblastoma (NB) subjects in the validation cohort. **A)** Associations between clinical characteristics and genomic alterations of 159 NB subjects in the validation cohort. The **horizontal axis** represents samples, and the **vertical axis** represents clinical characteristics (sex, age in months at diagnosis, International NB Staging System [INSS] stage, and outcome) and genetic alterations (copy number alterations and mutations). Each parameter is distinguished by the **indicated color**. *ATM* mutations were mutually exclusive with 11q loss of heterozygosity. In addition, the samples with mutations in DNA damage response (DDR)–associated genes, including *ATM*, were mutually exclusive. **B)** DDR-associated gene pathway and the frequency of genetic alterations in 159 NB tumor samples across the validation cohort. Genes located on chromosome 11q are colored in **yellow**; other DDR-associated genes are colored in **light blue**. The types of alterations and their frequencies are indicated to the **right of each gene**. LOH = loss of heterozygosity.

Downloaded from https://academic.oup.com/jnci/article/109/11/djx062/4096548 by guest on 24 April 2024

ARTICLE

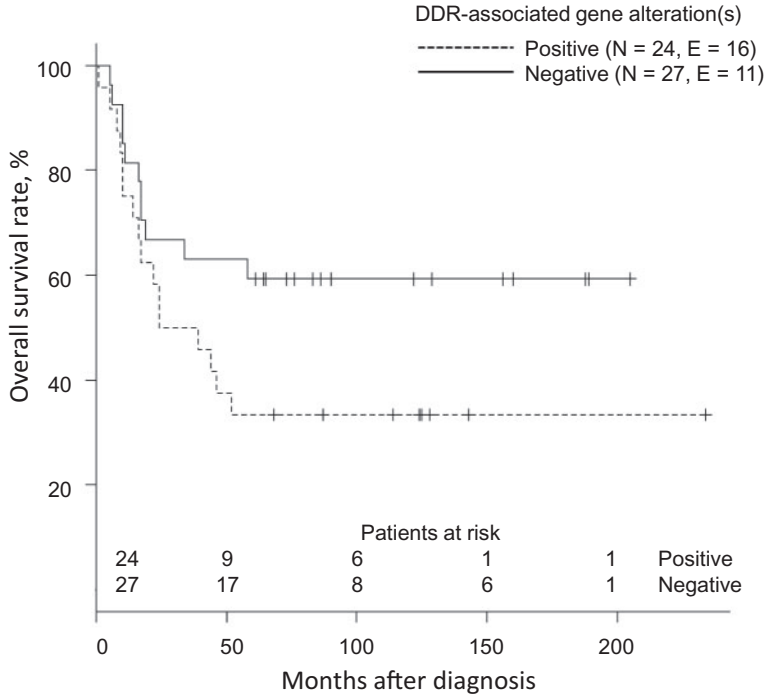

Figure 3. Kaplan-Meier curves of overall survival for neuroblastoma (NB) patients from the validation cohort (all stages). **Dashed and solid lines** indicate positive or negative DNA damage response–associated gene alteration, respectively. The 51 NB subjects were censored cases with five or more years of observation (n = 24) and the entire cohort of deaths (n = 27). The median observation period for the censored cases was 123 months (range = 61 – 234 months). The *P* value of the two-sided log-rank test is shown. E = events.

DDR-associated genes in six NB-derived cell lines (Supplementary Table 5, available online). In the fresh clinical samples from the validation cohort, we also investigated SNVs in the DDR-associated genes that are downstream of ATM and located within 11q 21 – 24 (*MRE11A, H2AFX, CHEK1*), as well as DDR-associated genes located on other chromosomes (*BARD1, BRCA1, TP53, CHEK2*). SNVs were observed at frequencies between 0.6% and 8.8% (Figure 2, A and B; Supplementary Figure 2 and Supplementary Table 6, available online). Intriguingly, SNVs in DDR-associated genes, including *ATM*, were mutually exclusive (Figure 2A). At least one SNV was identified in 26.4% (33/159) of fresh NB samples (Figure 2B). Overall, samples with SNVs and/or copy number alterations in these genes accounted for 48.4% (77/159) of all NB cases.

Survival of NB With DDR-Associated Gene Alterations

We compared survival of all stage cases (Figure 3) and cases in stages III and IV (Supplementary Figure 3, available online) and found that among these patients there was no difference in prognosis between those with and without DDR-associated gene alterations ($P = .08$ and $P = .41$, respectably).

Functional Analysis of Identified SNVs

Because *ATM* harbors various single nucleotide polymorphisms (SNPs) in approximately 5% of the population, we sequenced *ATM* and *BARD1* in control DNA from 171 healthy individuals to evaluate the consequence of SNVs identified in tumor samples. SNVs in *ATM* and *BARD1* were detected in 5.3% (9/171) and 1.2% (2/171), respectively (Supplementary Table 7, available online). To determine whether the rare SNVs identified in the discovery, validation, and healthy cohorts were functionally altered or represent neutral polymorphisms, we performed in vitro functional assays. ATM-defective cells exhibit radiation hypersensitivity; thus SNVs were subcloned into expression vectors and transduced into *ATM*-null fibroblasts to assess their functional effect on radiosensitivity. All SNVs identified in the NB cohort, except V1841I, failed to restore (or only partially restored) the hyperradiosensitivity phenotype of *ATM*-null cells, suggesting that these SNVs, except for V1841I, are functionally defective (Figure 4A). Although V1841I was identified as a somatic mutation and was expected to be functionally defective, V1841I is more likely to be a passenger mutation. Furthermore, two SNVs, S1455R and K2749I, were observed in both healthy control and tumor samples. Functional evaluation of these two SNVs revealed that complementation with either SNV moderately reversed radiosensitivity (Figure 4B). By contrast, all other SNVs originating from healthy control individual samples fully restored radiosensitivity, reflecting normal ATM function (Figure 4C).

DDR Activation in Fresh NB Samples

Unscheduled DNA replication driven by oncogenic stimuli activates DDR. We examined activation of ATM, as reflected by its auto-phosphorylation, using immunohistochemistry in 27 pathological specimens of fresh NB: eight stage I and II, 17 stage III and IV, and two stage IVS. Of these, 75% (6/8) of stage I and II and 100% (2/2) of IVS samples exhibited phospho-ATM and generic ATM staining, indicating the presence of double strand breaks induced by unscheduled DNA replication enforced by activating oncogenic stimuli. However, only 21.4% (3/14) of stage III and IV NB specimens exhibited ATM and phospho-ATM positivity ($P = .005$, stage I and II vs stage III and IV; $P = .01$, stage IVS

Downloaded from https://academic.oup.com/jnci/article/109/11/djx062/4096548 by guest on 24 April 2024

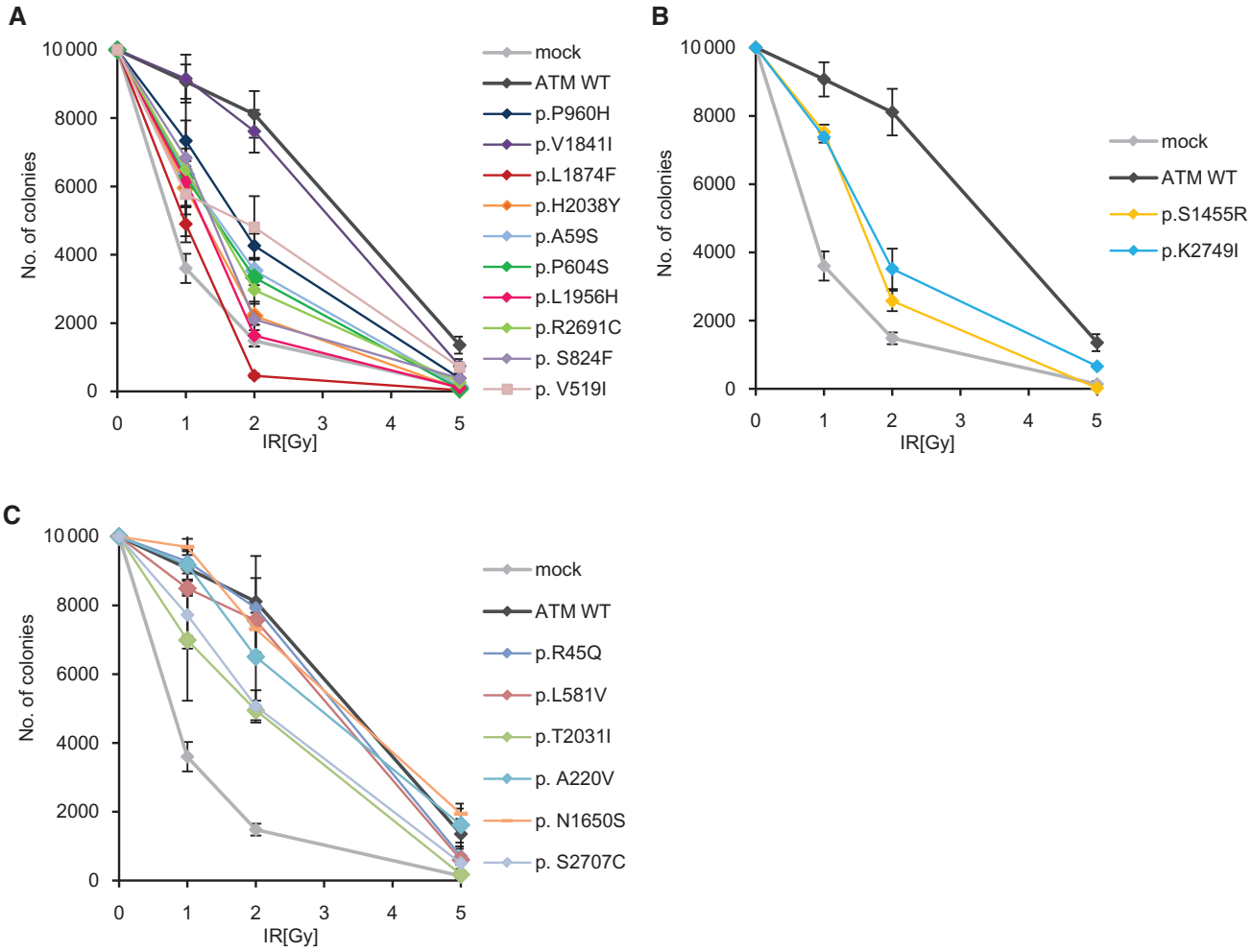

Figure 4. Clonogenic cell survival of *ATM* single nucleotide variant (SNV)–complemented cells challenged with X-irradiation. Cells complemented with mock, wild-type ATM, or ATM SNVs were X-irradiated at the indicated doses. Data are shown from three or six independent experiments. **A)** SNVs identified in fresh tumors and cell lines only. **B)** SNVs identified in both healthy control and fresh tumor samples. **C)** SNVs identified only in healthy controls. *ATM* wild-type-transduced and mock-transduced cells are shown as positive and negative controls, respectively. **Error bars** indicate standard deviation.

vs stage III and IV), suggesting loss, mutation, or inactivation of ATM in the latter samples (Figure 5, A and B).

Characterization of NB-Derived Cell Lines

Consistent with the results of genomic analysis, immunoblotting revealed that cell lines exhibiting haploid loss of the *ATM* gene locus exhibited reduced ATM protein expression (Figure 6A). To clarify the relationship between *ATM* gene alteration and ATM function in NB-derived cell lines, we investigated ATM-dependent DDR. ATM activity was evaluated in irradiated cells by measuring phosphorylation of the downstream substrate SMC1 because ATM levels varied between cell lines, whereas SMC1 expression was uniform. As anticipated, SMC1 phosphorylation was attenuated in clones with *ATM* haploinsufficiency, as well as in *ATM*-null GOTO cells. Notably, in the three clones that contained an intact *ATM* locus, CHP-134, IMR-32, and NB-9, SMC1 phosphorylation was also impaired. Among them, IMR-32 carried a homozygous V2716A *ATM* mutation due to UPD. By contrast, the ATM-competent lines SK-N-BE, SK-N-SH, and NB-69 exhibited normal responses (Figure 6B). Although the reason underlying the defective SMC1 phosphorylation in CHP-134 and NB-9 remains elusive, the majority of the NB-derived cell lines were functionally defective in the DDR regulated by ATM.

Sensitivity of NB Cells to PARP Inhibitors

PARP inhibitors (PARPi) induce synthetic lethality in HRR-defective cells (30,31). ATM is involved in HRR, and PARPi is therapeutically effective in ATM-deleted mantle cell lymphoma (32). MRE11, H2FX, and BARD1 also affect the HRR process, either directly or via ATM. Accordingly, we investigated the sensitivity of NB-derived cell lines to the PARP inhibitor olaparib. Except for SK-N-SH and SK-N-BE, which retain wild-type ATM and normal DDR (Figure 6B), 83.3% (10/12) of NB-derived cell lines exhibited elevated olaparib sensitivity (Figure 7A). Next, HRR activity was measured using DR-GFP assay. Confirming the previously published data (33), ATM inhibitor KU55933 treatment reduced GFP-positive cell number after I-SceI transduction, suggesting attenuated HRR efficiency of ATM-competent SK-N-BE cells ($P = .004$) (Figure 7B). In addition, most ATM mutants identified from fresh tumor samples, except for L1956H and R2691C, could not rescue PARPi sensitivity of ATM-null

Downloaded from https://academic.oup.com/jnci/article/109/11/djx062/4096548 by guest on 24 April 2024

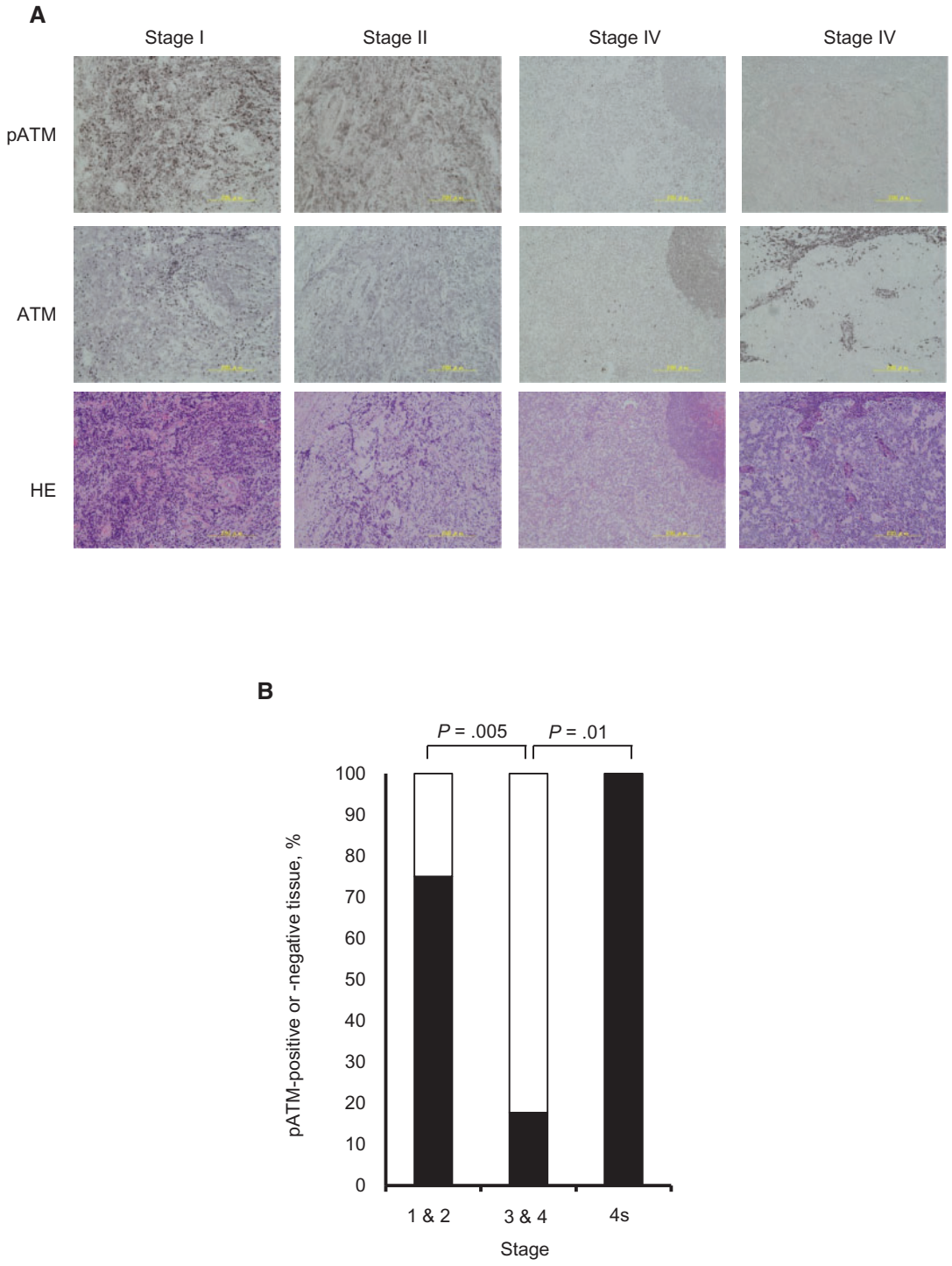

Figure 5. DNA damage response activation in fresh neuroblastoma (NB) tissue specimens. **A)** Immunohistochemistry of representative cases from stage I and II, as well as two representative cases from stage IV, is shown. **Scale bars** = 200 μm. **B)** Phospho-ATM (p-ATM)-positive tissue percentage in NB. Percent p-ATM-positive tissue is shown as either **white** (not detectable) or **black** (detectable) **bars**. *P* values were calculated using a two-sided Mann-Whitney U test. HE = hematoxylin and eosin staining.

SV40-transformed fibroblasts (Figure 7C). Next, we assessed olaparib sensitivity using in vivo xenografts of ATM-haploinsufficient SK-N-DZ and ATM-competent SK-N-SH cells in NSG mice. Tumor cell growth was markedly attenuated in the group receiving olaparib treatment only in mice with ATM-haploinsufficient SK-N-DZ xenografts (mean [SD] tumor volume of sham-treated vs olaprib-treated groups = 7377 [1451] m^3 vs 298 [312] m^3, $P = .001$, $n = 4$) (Figure 7, D and E). These experiments clearly show that NB with ATM dysfunction represents a candidate target for PARPi.

Downloaded from https://academic.oup.com/jnci/article/109/11/djx062/4096548 by guest on 24 April 2024

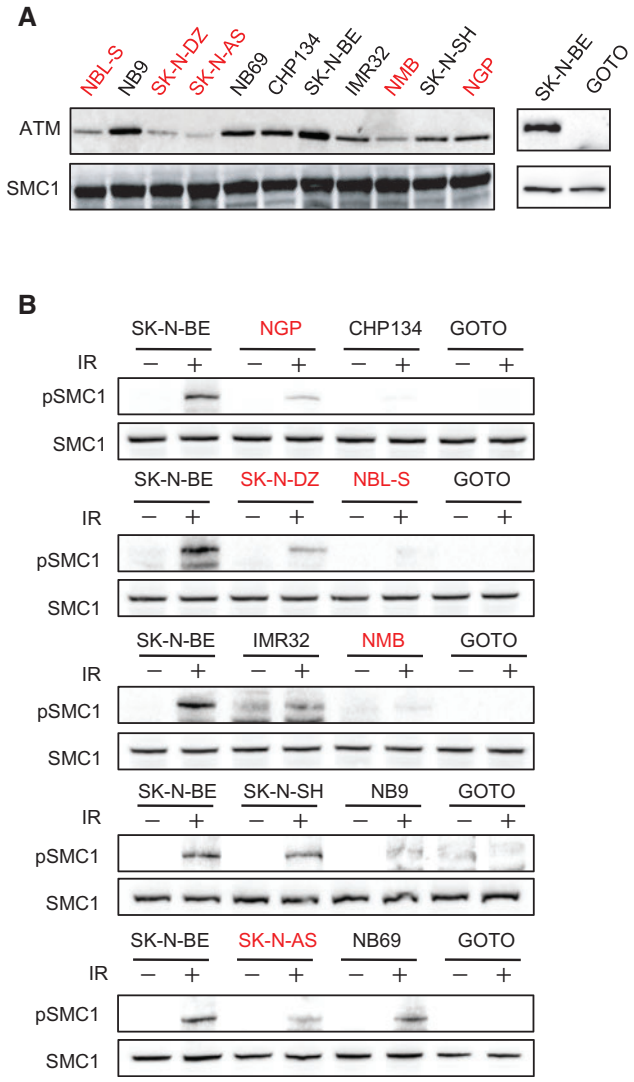

Figure 6. ATM expression and DNA damage response (DDR) after irradiation in neuroblastoma (NB)-derived cell lines. **A)** Immunoblot analysis of ATM expression. Expression of SMC1 is shown as a loading control. **B)** DDR activation in NB cells. Cells were irradiated (IR) at 2 Gy and harvested one hour after IR. Then, cells were lysed and subjected to immunoblotting to analyze phosphorylated SMC1, with SMC1 as the loading control.

Discussion

Ataxia telangiectasia and Nijmegen breakage syndrome are associated with a variety of tumors, including leukemias and lymphomas; however, NB has rarely been associated with chromosomal breakage syndromes (34,35), although several reports have described development of NB in Fanconi anemia (36–40). In the present study, we detected loss or imbalance of the *ATM* locus of fresh NB subjects. Mandriota et al. also reported that *ATM* deletions are present in 14 of 50 (28%) patients with NB and that progression of NB is promoted by silencing of ATM (41). Loss of *ATM* was linked with poor prognoses in mantle cell lymphoma and chronic lymphocytic leukemia (26,42). Therefore, prognostic significance based on *ATM* loss may be universally valuable across various tumors, including NB.

This study revealed that 7.2% of NB samples carry ATM SNVs. Some *ATM* SNVs are present at the germline level (Supplementary Table 2, available online). However, in this cohort, family history, such as that pertaining to cancer segregation or ataxia, was not obtained. Because most A-T-associated mutations are nonsense mutations, we anticipated that these patients would not present with classical A-T. Previously, biallelic missense mutation in the *ATM* gene was identified as responsible for adult-onset dystonia (43). Because NB develops at a relatively young age and is difficult to cure at advanced stages, it is possible that *ATM* germline SNVs also confer the potential risk of dystonia development later in life. *ATM* germline missense mutations contribute to cancer susceptibility (44–46). For example, rare *ATM* SNVs confer strong cancer predisposition in familial pancreatic cancer; however, familial pancreatic cancer with *ATM* SNVs is relatively rare (47,48). Previous whole-exome sequencing of 240 NB samples identified rare, potentially pathogenic, germline variants in *ALK*, *CHEK2*, *PINK1*, and *BARD1* (49); another study identified three *ATM* SNVs (4). Together with the results of the present study, these findings suggest that pathogenic germline variants of *ATM* and/or other DDR-associated molecules, including *BARD1*, are genetic risk factors for NB susceptibility.

Although most instances of 11q deletion do not overlap with *MYCN* amplification in NB, a relationship between MYC and ATM has been reported. Activation of MYC augments ATM-dependent DDR (50), and *DMAP1*, located at chromosome 1p, promotes *MYCN*-dependent ATM activation (51). In turn, the DDR plays a critical role in malignant transformation: specifically, ATM suppresses tumorigenesis in response to MYC (23,25). These data indicate that ATM functions as a tumor suppressor following *MYCN* amplification. Notably, *MYCN* overexpression induces expression of miR-421, which downregulates ATM expression in NB cells (52). These observations suggest that most cases of advanced NB exhibit downregulation of ATM, either directly because of 11q deletion or mediated by miR-421 in *MYCN*-amplified NB. Thus, we speculate that the ATM-dependent DDR response is suppressed to various extents in most cases of advanced NB. In addition, defects in other molecules associated with DDR, such as FANCM, FAN1, PALB2, MRE11A, and BARD1, were previously reported (49,53) and observed in the present study. Furthermore, most NB-derived cell lines exhibited increased sensitivity to PARPi. In the present study, CHP-134 and NB-9 exhibited attenuated phosphorylation of SMC1 after DNA damage and elevated PARPi sensitivity without ATM loss or mutation. It is likely that additional molecules involved in DDR, which were not identified in this study, may contribute to PARPi sensitivity. Indeed, *BRCA1*, *BRCA2*, and *BARD1* SNVs were detected in SK-N-DZ, CHP-134, and NB-69 (Supplementary Table 4, available online).

Our study is not without limitations. It remains unclear how and when the mutation of DDR-associated molecules, or loss of 11q, occurs during tumor development and progression. In this study, we could not compare the frequency of mutations in DDR-associated molecules or 11q loss between initial samples and relapsed or metastatic region. Maesechia et al. reported that 11q deletion was present from the early stage of tumor in stage IV NB, while 11q deletion occurred prior to 3p loss. This observation highlights the critical role of 11q deletion in stage IV tumors and suggests that structural 11q aberration confers tumor aggressiveness as a consequence of chromosome instability (54).

Multiple DDR-associated genes located at the 11q locus were deleted simultaneously. However, in our study, we could not examine how the combination of haploinsufficiency associates with tumor development. Actually, *Atm*, *Mre11a*, *Chek1*, or *H2afx* heterozygous knockout mice did not exhibit increased tumor

Downloaded from https://academic.oup.com/jnci/article/109/11/djx062/4096548 by guest on 24 April 2024
ARTICLE

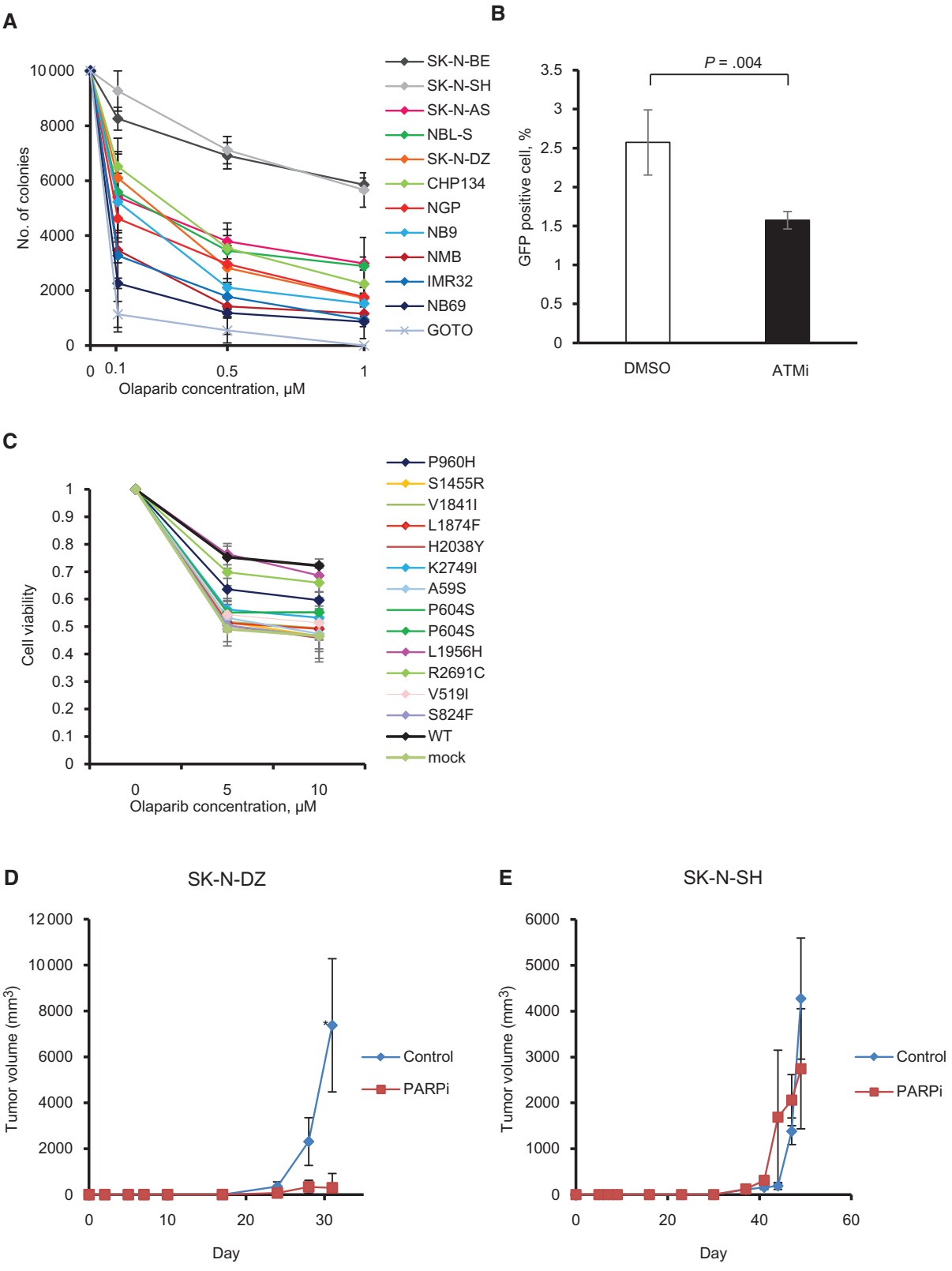

Figure 7. Sensitivity of neuroblastoma (NB) tumor cells to PARP inhibitor treatment. **A)** Clonogenic cell survival of various NB-derived cell lines. **B)** Cells were treated with DMSO (control) or 10 μM ATM inhibitor (KU-55933) immediately prior to the induction of DSBs via transfection with the I-SceI expression vector. After 72 hours, the percentage of GFP-positive cells was monitored by flow cytometry. **C)** Cell viability after olaparib treatment. ATM wild-type, mutant, or mock-transduced cells were plated at 1000 cells/100 μl. WST-8 assay was performed 72 hours after olaparib addition. **E)** In vivo tumorigenesis assay showing marked inhibition of SK-N-DZ tumor growth following olaparib treatment. **F)** As in **(E)**, except that SK-N-SH was transplanted. Four mice were used in each treatment group. **Error bars** represent standard deviation. *P* value was calculated using a two-sided Mann-Whitney U test.

Downloaded from https://academic.oup.com/jnci/article/109/11/djx062/4096548 by guest on 24 April 2024

susceptibility. It is curious to examine *Atm, Mre11a, Chek1*, and *H2afx* quad heterozygous knockout mice.

Several reports have described PARP inhibition in NB but did not extensively investigate DDR. Norris et al. reported that olaparib inhibits the growth of pediatric solid tumor cell lines, including those derived from NB. The addition of olaparib to DNA-damaging agents results in additive or synergistic interactions (55). Muller et al. proposed that a combination of the PARP inhibitor MK-4827 and radiation may be an effective therapy for children with high-risk NB (56). Preclinical data suggest that PARPi may potentiate the effects of radiotherapy not only in NB, but also in several other tumor types (57). Combination chemotherapy using PARPi with alkylating agents, platinum agents, or radiotherapy may effectively suppress NB progression. Therefore, we believe that the use of PARPi represents a promising therapeutic approach for specifically targeting HRR-defective NB.

Funding

This work was supported by the Ministry of Education, Culture, Sports, Science, and Technology (MEXT) Grants-in-Aid for Scientific Research (23390271 to MT and SM; 26464568 to RT; 25253095 to JT); Japan Society for the Promotion of Science; Grants-in-Aid for Scientific Research and P-DIRECT; Ministry of Health, Labor and Welfare (MHLW); Health and Labor Sciences Research Grants; Research on Measures for Intractable Diseases; Research on Health Sciences Focusing on Drug Innovation; Japan Agency for Medical Research and Development (AMED); Japan Science and Technology Agency (JST); Core Research for Evolutional Science and Technology (CREST); Japan Health Sciences Foundation; P-CREATE; and the Princess Takamatsu Cancer Research Fund.

Notes

Authors: Masatoshi Takagi*, Misa Yoshida*, Yoshino Nemoto*, Hiroyuki Tamaichi, Rika Tsuchida, Masafumi Seki, Kumiko Uryu, Noriko Hoshino, Rina Nishii, Satoshi Miyamoto, Masahiro Saito, Toshiaki Shimizu, Ryoji Hanada, Hideo Kaneko, Toshiyuki Fukao, Takatoshi Koyama, Yuichi Shiraishi, Kenichi Chiba, Hiroko Tanaka, Satoru Miyano, Yusuke Sato, Yoichi Fujii, Keisuke Kataoka, Yusuke Okuno, Kenichi Yoshida, Tomohiro Morio, Akira Oka, Miki Ohira, Yasuhide Hayashi, Akira Nakagawara, Seishi Ogawa, Shuki Mizutani, Junko Takita

Affiliations of authors: Department of Pediatrics and Developmental Biology (MT, YN, RT, RN, SMiyam, TM, SMiz) and Graduate School of Health Care Sciences, Laboratory Molecular Genetics of Hematology (TK), Tokyo Medical and Dental University, Tokyo, Japan; Department of Pediatrics, Graduate School of Medicine (MY, MSe, KU, NH, AO, JT), Department of Pediatric Surgery, Graduate School of Medicine (NH), Laboratory of DNA Information Analysis, Human Genome Center, Institute of Medical Science (YSh, KC, SMiyan), and Laboratory of Sequence Analysis, Human Genome Center, Institute of Medical Science (HTan, SMiyan), The University of Tokyo, Tokyo, Japan; Department of Pediatrics and Adolescent Medicine, School of Medicine, Juntendo University, Tokyo, Japan (HTam, MSa, TS); Department of Pediatric Hematology/Oncology, Saitama Children's Medical Center, Saitama, Japan (RH); Department of Pediatrics, Nagara Medical Center, Gifu, Japan (HK); Department of Pediatrics, Gifu University, Gifu, Japan (TF); Department of Pathology and Tumor Biology, Kyoto University, Kyoto, Japan (YSa, YF, KK, YO, KY, SO); Department of Pediatrics, Nagoya University Graduate School of Medicine, Nagoya, Japan (YO); Division of Cancer Genomics, Saitama Cancer Center Research Institute, Saitama, Japan (MO); Division of Cancer Genomics, Chiba Cancer Center, Chiba, Japan (MO, AN); Gunma Children's Medical Center, Gunma, Japan (YH); Saga Medical Center, Saga, Japan (AN).

The funders had no role in the design of the study; the collection, analysis, or interpretation of the data; the writing of the manuscript; or the decision to submit the manuscript for publication.

We are grateful to Ms. Matsumura, Ms. Hoshino, Ms. Yin, Ms. Saito, Ms. Nakamura, Ms. Mizota, Ms. Sato, and Ms. Nishikawa for their excellent technical assistance.

References

1. Maris JM. Recent advances in neuroblastoma. *N Engl J Med*. 2010;362(23):2202–2211.
2. Chen Y, Takita J, Choi YL, et al. Oncogenic mutations of ALK kinase in neuroblastoma. *Nature*. 2008;455(7215):971–974.
3. Mosse YP, Laudenslager M, Longo L, et al. Identification of ALK as a major familial neuroblastoma predisposition gene. *Nature*. 2008;455(7215):930–935.
4. Capasso M, Devoto M, Hou C, et al. Common variations in BARD1 influence susceptibility to high-risk neuroblastoma. *Nat Genet*. 2009;41(6):718–723.
5. Maris JM, Mosse YP, Bradfield JP, et al. Chromosome 6p22 locus associated with clinically aggressive neuroblastoma. *N Engl J Med*. 2008;358(24):2585–2593.
6. Wang K, Diskin SJ, Zhang H, et al. Integrative genomics identifies LMO1 as a neuroblastoma oncogene. *Nature*. 2011;469(7329):216–220.
7. Spitz R, Hero B, Ernestus K, Berthold F. Deletions in chromosome arms 3p and 11q are new prognostic markers in localized and 4s neuroblastoma. *Clin Cancer Res*. 2003;9(1):52–58.
8. Attiyeh EF, London WB, Mosse YP, et al. Chromosome 1p and 11q deletions and outcome in neuroblastoma. *N Engl J Med*. 2005;353(21):2243–2253.
9. George RE, Attiyeh EF, Li S, et al. Genome-wide analysis of neuroblastomas using high-density single nucleotide polymorphism arrays. *PLoS One*. 2007;2(2):e255.
10. Mertens F, Johansson B, Hoglund M, Mitelman F. Chromosomal imbalance maps of malignant solid tumors: A cytogenetic survey of 3185 neoplasms. *Cancer Res*. 1997;57(13):2765–2780.
11. Guo C, White PS, Weiss MJ, et al. Allelic deletion at 11q23 is common in MYCN single copy neuroblastomas. *Oncogene*. 1999;18(35):4948–4957.
12. Michels E, Hoebeeck J, De Preter K, et al. CADM1 is a strong neuroblastoma candidate gene that maps within a 3.72 Mb critical region of loss on 11q23. *BMC Cancer*. 2008;8:173.
13. Ando K, Ohira M, Ozaki T, et al. Expression of TSLC1, a candidate tumor suppressor gene mapped to chromosome 11q23, is downregulated in unfavorable neuroblastoma without promoter hypermethylation. *Int J Cancer*. 2008;123(9):2087–2094.
14. Morrison C, Sonoda E, Takao N, Shinohara A, Yamamoto K, Takeda S. The controlling role of ATM in homologous recombinational repair of DNA damage. *EMBO J*. 2000;19(3):463–471.
15. Golding SE, Rosenberg E, Khalil A, et al. Double strand break repair by homologous recombination is regulated by cell cycle-independent signaling via ATM in human glioma cells. *J Biol Chem*. 2004;279(15):15402–15410.
16. Bryant HE, Helleday T. Inhibition of poly (ADP-ribose) polymerase activates ATM which is required for subsequent homologous recombination repair. *Nucleic Acids Res*. 2006;34(6):1685–1691.
17. Beucher A, Birraux J, Tchouandong L, et al. ATM and Artemis promote homologous recombination of radiation-induced DNA double-strand breaks in G2. *EMBO J*. 2009;28(21):3413–3427.
18. Kastan MB, Bartek J. Cell-cycle checkpoints and cancer. *Nature*. 2004;432(7015):316–323.
19. Bartkova J, Horejsi Z, Koed K, et al. DNA damage response as a candidate anti-cancer barrier in early human tumorigenesis. *Nature*. 2005;434(7035):864–870.
20. Gorgoulis VG, Vassiliou LV, Karakaidos P, et al. Activation of the DNA damage checkpoint and genomic instability in human precancerous lesions. *Nature*. 2005;434(7035):907–913.
21. Horibe S, Takagi M, Unno J, et al. DNA damage check points prevent leukemic transformation in myelodysplastic syndrome. *Leukemia*. 2007;21(10):2195–2198.
22. Takagi M, Sato M, Piao J, et al. ATM-dependent DNA damage-response pathway as a determinant in chronic myelogenous leukemia. *DNA Repair (Amst)*. 2013;12(7):500–507.

Downloaded from https://academic.oup.com/jnci/article/109/11/djx062/4096548 by guest on 24 April 2024

ARTICLE

23. Pusapati RV, Rounbehler RJ, Hong S, et al. ATM promotes apoptosis and suppresses tumorigenesis in response to Myc. *Proc Natl Acad Sci U S A*. 2006; 103(5):1446–1451.
24. Campaner S, Amati B. Two sides of the Myc-induced DNA damage response: From tumor suppression to tumor maintenance. *Cell Div*. 2012;7(1):6.
25. Maclean KH, Kastan MB, Cleveland JL. Atm deficiency affects both apoptosis and proliferation to augment Myc-induced lymphomagenesis. *Mol Cancer Res*. 2007;5(7):705–711.
26. Cuneo A, Bigoni R, Rigolin GM, et al. Acquired chromosome 11q deletion involving the ataxia teleangiectasia locus in B-cell non-Hodgkin's lymphoma: Correlation with clinicobiologic features. *J Clin Oncol*. 2000;18(13):2607–2614.
27. Mermel CH, Schumacher SE, Hill B, Meyerson ML, Beroukhim R, Getz G. GISTIC2.0 facilitates sensitive and confident localization of the targets of focal somatic copy-number alteration in human cancers. *Genome Biol*. 2011; 12(4):R41.
28. Demuth I, Dutrannoy V, Marques W Jr, et al. New mutations in the ATM gene and clinical data of 25 AT patients. *Neurogenetics*. 2011;12(4):273–282.
29. Scott SP, Bendix R, Chen P, Clark R, Dork T, Lavin MF. Missense mutations but not allelic variants alter the function of ATM by dominant interference in patients with breast cancer. *Proc Natl Acad Sci U S A*. 2002;99(2):925–930.
30. Bryant HE, Schultz N, Thomas HD, et al. Specific killing of BRCA2-deficient tumours with inhibitors of poly(ADP-ribose) polymerase. *Nature*. 2005; 434(7035):913–917.
31. Farmer H, McCabe N, Lord CJ, et al. Targeting the DNA repair defect in BRCA mutant cells as a therapeutic strategy. *Nature*. 2005;434(7035):917–921.
32. Weston VJ, Oldreive CE, Skowronska A, et al. The PARP inhibitor olaparib induces significant killing of ATM-deficient lymphoid tumor cells in vitro and in vivo. *Blood*. 2010;116(22):4578–4587.
33. Bakr A, Oing C, Kocher S, et al. Involvement of ATM in homologous recombination after end resection and RAD51 nucleofilament formation. *Nucleic Acids Res*. 2015;43(6):3154–3166.
34. Antonio JR, Fett-Conte AC, Thome JA, et al. Familial Bloom's syndrome associated with neuroblastoma. *Rev Paul Med*. 1990;108(1):9–16.
35. Hiel JA, Weemaes CM, van den Heuvel LP, et al. Nijmegen breakage syndrome. The International Nijmegen Breakage Syndrome Study Group. *Arch Dis Child*. 2000;82(5):400–406.
36. Halperin EC. Neonatal neoplasms. *Int J Radiat Oncol Biol Phys*. 2000;47(1): 171–178.
37. Berrebi D, Lebras MN, Belarbi N, et al. Bilateral adrenal neuroblastoma and nephroblastoma occurring synchronously in a child with Fanconi's anemia and VACTERL syndrome. *J Pediatr Surg*. 2006;41(1):e11–e14.
38. Serra A, Eirich K, Winkler AK, et al. Shared copy number variation in simultaneous nephroblastoma and neuroblastoma due to Fanconi Anemia. *Mol Syndromol*. 2012;3(3):120–130.
39. Compostella A, Toffolutti T, Soloni P, Dall'Igna P, Carli M, Bisogno G. Multiple synchronous tumors in a child with Fanconi anemia. *J Pediatr Surg*. 2010;45(2): e5–e8.
40. Bissig H, Staehelin F, Tolnay M, et al. Co-occurrence of neuroblastoma and nephroblastoma in an infant with Fanconi's anemia. *Hum Pathol*. 2002;33(10): 1047–1051.
41. Mandriota SJ, Valentijn LJ, Lesne L, et al. Ataxia-telangiectasia mutated (ATM) silencing promotes neuroblastoma progression through a MYCN independent mechanism. *Oncotarget*. 2015;6(21):18558–18576.
42. Skowronska A, Parker A, Ahmed G, et al. Biallelic ATM inactivation significantly reduces survival in patients treated on the United Kingdom Leukemia Research Fund Chronic Lymphocytic Leukemia 4 trial. *J Clin Oncol*. 2012; 30(36):4524–4532.
43. Saunders-Pullman R, Raymond D, Stoessl AJ, et al. Variant ataxia-telangiectasia presenting as primary-appearing dystonia in Canadian Mennonites. *Neurology*. 2012;78(9):649–657.
44. Gatti RA, Tward A, Concannon P. Cancer risk in ATM heterozygotes: A model of phenotypic and mechanistic differences between missense and truncating mutations. *Mol Genet Metab*. 1999;68(4):419–423.
45. Tavtigian SV, Chenevix-Trench G. Growing recognition of the role for rare missense substitutions in breast cancer susceptibility. *Biomark Med*. 2014;8(4): 589–603.
46. Stankovic T, Stewart GS, Byrd P, Fegan C, Moss PA, Taylor AM. ATM mutations in sporadic lymphoid tumours. *Leuk Lymphoma*. 2002;43(8):1563–1571.
47. Roberts NJ, Jiao Y, Yu J, et al. ATM mutations in patients with hereditary pancreatic cancer. *Cancer Discov*. 2012;2(1):41–46.
48. Roberts NJ, Norris AL, Petersen GM, et al. Whole genome sequencing defines the genetic heterogeneity of familial pancreatic cancer. *Cancer Discov*. 2016; 6(2):166–175.
49. Pugh TJ, Morozova O, Attiyeh EF, et al. The genetic landscape of high-risk neuroblastoma. *Nat Genet*. 2013;45(3):279–284.
50. Guerra L, Albihn A, Tronnersjo S, et al. Myc is required for activation of the ATM-dependent checkpoints in response to DNA damage. *PLoS One*. 2010; 5(1):e8924.
51. Yamaguchi Y, Takenobu H, Ohira M, et al. Novel 1p tumour suppressor Dnmt1-associated protein 1 regulates MYCN/ataxia telangiectasia mutated/p53 pathway. *Eur J Cancer*. 2014;50(8):1555–1565.
52. Hu H, Du L, Nagabayashi G, Seeger RC, Gatti RA. ATM is down-regulated by N-Myc-regulated microRNA-421. *Proc Natl Acad Sci U S A*. 2010;107(4): 1506–1511.
53. Molenaar JJ, Koster J, Zwijnenburg DA, et al. Sequencing of neuroblastoma identifies chromothripsis and defects in neuritogenesis genes. *Nature*. 2012; 483(7391):589–593.
54. Masecchia S, Coco S, Barla A, Verri A, Tonini GP. Genome instability model of metastatic neuroblastoma tumorigenesis by a dictionary learning algorithm. *BMC Med Genomics*. 2015;8:57.
55. Norris RE, Adamson PC, Nguyen VT, Fox E. Preclinical evaluation of the PARP inhibitor, olaparib, in combination with cytotoxic chemotherapy in pediatric solid tumors. *Pediatr Blood Cancer*. 2014;61(1):145–150.
56. Mueller S, Bhargava S, Molinaro AM, et al. Poly (ADP-Ribose) polymerase inhibitor MK-4827 together with radiation as a novel therapy for metastatic neuroblastoma. *Anticancer Res*. 2013;33(3):755–762.
57. Powell C, Mikropoulos C, Kaye SB, et al. Pre-clinical and clinical evaluation of PARP inhibitors as tumour-specific radiosensitisers. *Cancer Treat Rev*. 2010; 36(7):566–575.

Downloaded from https://academic.oup.com/jnci/article/109/11/djx062/4096548 by guest on 24 April 2024